Research Article

Zakaria Tabia, Sihame Akhtach, Khalil El Mabrouk*, Meriame Bricha, Khalid Nouneh, and Anbalagan Ballamurugan

Tantalum doped SiO_2-CaO-P_2O_5 based bioactive glasses: Investigation of *in vitro* bioactivity and antibacterial activities

https://doi.org/10.1515/bglass-2020-0002
Received Jan 27, 2020; revised Apr 13, 2020; accepted Apr 25, 2020

Abstract: Multifunctionality can be achieved for bioactive glasses by endowing them with multiple other properties along with bioactivity. One way to address this topic is by doping these glasses with therapeutic metallic ions. In this work, we put under investigation a series of bioactive glasses doped with tantalum. We aim to study the effect of tantalum, on the structure, bioactivity and antibacterial property of a ternary bioactive glass composition based on SiO_2-CaO-P_2O_5. Fourier Transformed Infrared Spectroscopy (FTIR), X-Ray Diffraction (XRD) and Electron Scanning Microscopy (SEM) were used to assess the structural and morphological properties of these glasses and monitor their changes after *in vitro* acellular bioactivity test. Antibacterial activity was tested against gram positive and negative bacteria. Characterization results confirmed the presence of calcium carbonate crystallites along with the amorphous silica matrix. The assessment of bioactivity in SBF indicated that all compositions showed a fast bioactive response after only six hours of immersion period. However, analytical characterization revealed that tantalum introduced a slight latency in hydroxyapatite deposition at higher concentrations (0.8-1 %mol). Antibacterial test showed that tantalum ions had an inhibition effect on the growth of *E. coli* and *S. aureus*. This effect was more pronounced in compositions where mol% of tantalum is superior to 0.4%. These results proved that tantalum could be used, in intermediate proportions, as a promising multifunctional dopant element in bioactive glasses for bone regeneration applications.

Keywords: tantalum; bioactive glass; bioactivity; antibacterial property, bone regeneration

1 Introduction

Biomaterials for bone regeneration are one of the most active research fields nowadays. The aim is to conceptualize and study new materials that can elicit promising biological and mechanical responses for stimulating and withstanding bone regeneration [1]. In the way of the endeavor to search the ideal biomaterial for bone healing, several breakthroughs have been made, among which the discovery of bioactive glasses by Professor L. Hench in 1969 [2, 3]. Since then, these inorganic materials have had, themselves, major advancements. Beginning with the introduction of sol-gel as a synthesis method [4] and its combination with supra-molecular chemistry to produce mesoporous materials through evaporation induced self-assembly (EISA) [5, 6], bioactive glasses have become a research field of its particular interest.

Two characteristics considered of utmost importance for biomaterials in general, and bioactive glasses in particular, are bioactivity and antibacterial property [7, 8]. Bioactive glasses make excellent candidates to be used as multifunctional materials that can stimulate new bone formation along with being anti-infective [9]. From a clinical point of view, experts have always seen bacterial infections as a major challenge for tissue regeneration and repair as they can lead to implant failure and prolonged healing of the bone defect [10, 11]. These infections which arise mainly from nosocomial contamination during surgery

***Corresponding Author: Khalil El Mabrouk:** Euromed Research Center, Euromed Engineering Faculty, Euromed University of Fes, Eco-Campus, Meknes Road, 30 030, Fes, Morocco; Email: k.elmabrouk@ueuromed.org; Tel: +212 662 054 920; Fax: +212 537 716 040

Zakaria Tabia: Euromed Research Center, Euromed Engineering Faculty, Euromed University of Fes, Eco-Campus, Meknes Road, 30 030, Fes, Morocco; Laboratory of Physics and Condensed Matter, Department of Physics, Ibn Tofail University, Kenitra, Morocco
Sihame Akhtach, Meriame Bricha: Euromed Research Center, Euromed Engineering Faculty, Euromed University of Fes, Eco-Campus, Meknes Road, 30 030, Fes, Morocco
Khalid Nouneh: Laboratory of Physics and Condensed Matter, Department of Physics, Ibn Tofail University, Kenitra, Morocco
Anbalagan Ballamurugan: Department of Nanoscience and Technology, Bharathiar Coimbatore, Tamil Nadu, India

will lead eventually to increase in the period of hospitalization, medication costs and the risk of patients' morbidity [12]. The most prevalent pathogens causing infections in medical devices are *Staphylococcus aureus*, and *Staphylococcus epidemidis* [10]. Others like *Escherichia coli* and *Pseudomonas aeruginosa* are also detected but their prevalence accounts for less than 7% in medical device infections [10]. The formation of protective biofilm and the organization of these pathogens into microcolonies, enable them to persist in the aggressive host site environment [13]. Furthermore, the seriousness of bacteria colonization arises not only from this latter but also from the ability of these microorganisms to develop resistance against antibiotics [14]. This ability originates from the adaptation of these microorganisms to common therapeutic molecules. In this sense, multifunctional biomaterials that possess intrinsic anti-infective properties are of high importance.

One way to achieve this multifunctionality is by doping bioactive glasses with metallic elements [15]. Magnesium [16, 17], strontium [18], copper [19], silver [20] and lithium [21] all have been thoroughly used as dopants to enhance the biological properties of SiO_2-CaO or SiO_2-CaO-P_2O_5 based glasses. For example, strontium stimulates osteoblast differentiation and proliferation and enhances ALP activity [22–24]. Copper has an angiogenesis enhancement effect [25], whereas silver has proved its use as an antibacterial agent [26, 27]. Other emerging elements such as gallium [28], cerium [29], and tantalum [30] have been also studied as dopants in bioactive glasses. Among these, tantalum is being increasingly investigated for application in the biomedical field. Since tantalum is corrosion-resistant, biocompatible and bioactive [31], it is exploited as a coating material to enhance the surface properties of metallic implants [32, 33]. This element is also used to fabricate orthopedic implants mainly because of its osteointegration property through an apatite layer formed on its surface in early bioactivity stages [34]. Vascular clips and cranioplasty plates are also among its uses in clinical practices.

Tantalum doped bioactive glasses were first reported through RKKP composition in which Ta_2O_5 [35, 36]. In recent reports, Alhalawani *et al.* [30, 37] investigated the effect of ZnO substitution by Ta_2O_5 on the physical and chemical properties of a multicomponent glass. They found that incorporation of Ta induced structural changes in the glass network, which in turn affected the thermal properties and glass solubility. Cordeiro *et al.* [38] studied Ta_2O_5 doped phosphate glasses. Their results showed that tantalum induced higher connectivity of the glass network, which resulted in a higher glass transition temperature. In all these studies [30, 35–38], glasses were prepared mainly by the melt-quench method. It is worth noting that sol-gel was also used for RKKP synthesis [39–41]. However, to the best of our knowledge, there is only one study in which tantalum doped glasses were prepared by EISA combined to sol-gel method [42]. In this study, tantalum incorporation affected the properties of 85S mesoporous bioactive glass by increasing the number of bridging oxygen and causing a reduction in the glass textural properties, *i.e.* surface area and pore volume. It was also found that Ta doped 85S can be used as a homeostatic agent [42]. According to above-mentioned literature [30, 35–42], the direct effect of tantalum on *in vitro* bioactivity and antibacterial property of bioactive glasses was not investigated and was discarded. In the present work, we report the synthesis of a tantalum doped bioactive glass series by EISA method as well as its structural characterization. We also investigate the effect of tantalum-doping on the bioactivity and antibacterial property against two relevant pathogenic bacteria, *E. coli* and *S. aureus*.

2 Materials and methods

2.1 Synthesis of bioactive glasses

For the synthesis of bioactive glass powders, the following chemical products were used as received without any further purification: ethanol (99.9%, BioSmart), hydrochloric acid (37%, VWR Chemicals), triblock copolymer pluronic L-81 (Mn~2800, Sigma Aldrich), tetraethyl orthosilicate (TEOS, 99%, VWR Chemicals), triethyl phosphate (TEP, 98.8%, Sigma Aldrich), calcium nitrate tetrahydrate (99%, Solvachim) and tantalum (V) ethoxide (99%, Alfa Aesar).

Evaporation induced self-assembly (EISA) was used to prepare bioactive glass 58S series doped with tantalum [6]. The molar nominal composition of the present series is 58% SiO_2 + 37% CaO + (5-x)% P_2O_5 + x% Ta_2O_5. Briefly, 5 grams of non-ionic surfactant pluronic L-81 was added to a mixture of ethanol (60g) and 0.5 M HCl (1g). After 30 minutes under magnetic stirring, TEOS (4.8g), TEP, tantalum ethoxide and Calcium nitrate (3.4g) were added in that order with 30 minutes between each component. The solution was kept under magnetic stirring for another 24 hours. Afterward, the solution was poured in Petri dishes and maintained at room temperature for 24 hours to undergo gelation. Next, samples were introduced in the oven at 40°C for 7 days for aging. Dried samples were calcined at 600°C for 6 hours. All compositions prepared in this work are shown in Table 1 as molar percentages.

Table 1: Molar composition of bioactive glasses in the 58S-Ta series [16]

Label	SiO_2	CaO	P_2O_5	Ta_2O_5
58S	0.58	0.37	0.05	0
58S0.2	0.58	0.37	0.048	0.002
58S0.4	0.58	0.37	0.046	0.004
58S0.6	0.58	0.37	0.044	0.006
58S0.8	0.58	0.37	0.042	0.008
58S1	0.58	0.37	0.04	0.01

2.2 Initial characterization

Thermogravimetric analysis was performed using a Q500-TA Instrument apparatus to determine the appropriate calcination temperature. Dried samples were heated from room temperature to 1000°C under air atmosphere at a heating rate of 10°C/min.

Structural features of calcined samples were assessed with Fourier Transformed Infrared Spectroscopy (FTIR) and X-Ray Diffraction (XRD). FTIR spectra of all compositions were obtained in Attenuated Total Reflection mode (ATR) using a Perkin-Elmer IS50 spectrometer. The spectra were acquired between 400 and 4000 cm^{-1} at a resolution of 4 cm^{-1}. XRD patterns were collected on an X-pert X-ray diffractometer. Cu-Kα was used as X-ray radiation, which was generated under voltage and current of 45 kV and 40 mA, respectively. The data were collected for 2θ ranging from 10 to 60°.

The elementary composition of the bioactive glass powders was assessed using Inductively Coupled Plasma Atomic Emission Spectroscopy (ICP-AES). The analysis was performed in triplicate on a HORIBA Jobin Yvon-Ultima 2 apparatus.

Surface morphology was assessed using Scanning Electron Microscopy on IEM 11+ Inovenso microscope under high vacuum mode and voltage of 15 kV. EDX spectra were also generated.

2.3 Acellular bioactivity

Acellular bioactivity was tested in simulated body fluid (SBF), which is a solution with an ionic composition similar to human blood plasma (see Table 2). It was prepared according to the protocol described by Kokubo *et al.* [43]. For the test, 50 mg of glass powder was dispersed in SBF with a ratio of 1 mg/ml and incubated at 37°C under minimal agitation. After each selected time point, solutions were filtered and their pH was measured. Powders were collected, dried and analyzed with FTIR, XRD and SEM to assess their apatite forming ability.

Table 2: Ionic concentration of human blood plasma and SBF [16]

Ion	Concentration (mM)	
	Blood Plasma	SBF
Na^+	142	142
K^+	5	5
Mg^+	1.5	1.5
Ca^{2+}	2.5	2.5
Cl^-	103	147.8
HCO^{3-}	27	4.2
HPO_4^{2-}	1	1
SO_4^{2-}	0.5	0.5
pH	7.2-7.4	7.2-7.4

2.4 Antibacterial activity

The antibacterial activity of the 58S-Ta series was studied against two strains, *Escherichia coli* (Gram-negative) and *Staphylococcus aureus* (Gram-positive) using the plate counting method [26, 44]. Before performing the test, all powders were sterilized with UV radiation. The inoculum was prepared in Lysogenic broth (LB) and was adjusted to about 10^8 CFU/ml by comparing its turbidity to that of 0.5 McFarland barium phosphate standard solution. Then diluted at a final concentration of 10^5 CFU/ml. Solutions of bioactive glass powders (10 mg/ml) were prepared in LB medium. Next, 10µl of the inoculum was added to 1 ml of BG solutions and incubated at 37°C for 8 hours. After incubation, the solutions were diluted with decimal series and 0.1 ml of each solution was platted on PCA agar. The plates were then cultured at 37°C for 16 hours. Positive and negative controls were also prepared for comparison purposes. All tests were performed in triplicate. For each composition, the number of viable cells was counted and expressed as the number of colony-forming units (CFU/ml). The antibacterial activity was determined by calculating the strain viability percentage using the following equation:

$$Strain\ Viability\ \% = \frac{CFU_S}{CFU_P} * 100$$

Where:

- CFU_S is the number of *CFU* counted in samples;
- CFU_P is the number of *CFU* counted in positive control.

3 Results and discussion

3.1 Initial characterization

A preliminary characterization was conducted to assess the structural and morphological properties of the 58S-Ta series. Thermogravimetric analysis results are depicted in Figure 1. The thermograms indicate the presence of three weight losses. The first one, which ends at 175°C, is related to the evaporation of ethanol and departure of physically adsorbed water. The second weight loss is attributed to the decomposition of surfactant molecules together with the loss of nitrates from the calcium precursor. Bérubé *et al.* [45] studied the calcination of SBA-15 mesoporous silica. They found that decomposition of pluronic began at relatively low temperature (175°C) whereas complete elimination of the surfactant molecules was achieved at temperatures higher than 500°C. Lastly, a slight weight loss can be observed between 500 and 620°C. It can be attributed to a rearrangement of atoms that might have induced a structural change in studied powder.

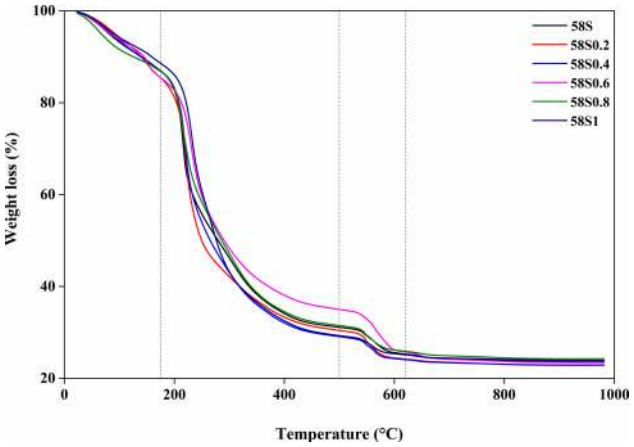

Figure 1: Thermogravimetric analysis of all six compositions in the 58S-Ta series

Prepared bioglass powders were first characterized using FTIR spectroscopy (Figure 2). The patterns reveal the presence of two distinct phases. The first one is assigned to the silica network. It is highlighted by the presence of four silica absorption bands [46]. Si-O-Si asymmetric stretching situated at 1024 cm^{-1}, Si-O stretching of non-bridging oxygen at 938 cm^{-1}, Si-O-Si bending at 421 cm^{-1} and symmetric stretching of Si-O-Si at around 812 cm^{-1}, which is superimposed with the Si-O band. Interestingly, the patterns also reveal the presence of bands relative to C-O vibration modes. These bands are located at 1521, 1410, 873 and 712 cm^{-1} and can be assigned to C-O vibration in a carbonate phase. Additional bands at 3373 and 1636 cm^{-1} are identified as vibration modes of O-H bonds. The FTIR spectra showed a significant change with respect to tantalum content in the glass composition. It can be noticed that the band assigned to the Si-O-Si asymmetric stretching slightly shifted to lower wavenumbers and decreased in intensity with the increase of tantalum content. Mendonca *et al.* [42] synthesized a series of mesoporous bioactive glass doped with tantalum. Their FTIR analysis showed a decrease in intensity of the characteristic band relative to Si-O with increasing tantalum content in the glass composition. This behavior was explained by the fact that tantalum incorporation induced a replacement of Si-O-Si by Si-O-Ta bonds.

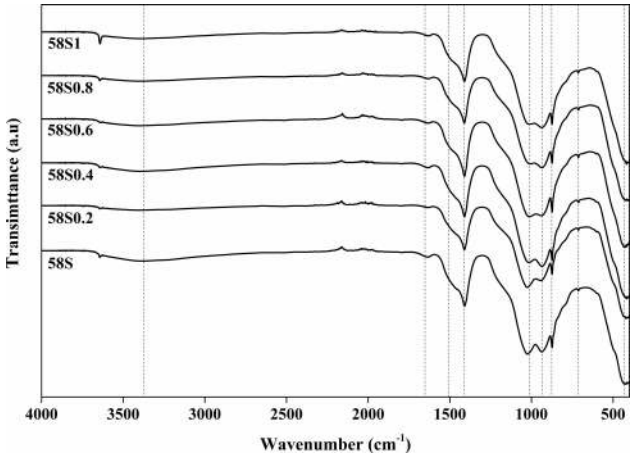

Figure 2: FTIR spectra of samples after heat treatment at 600°C

The XRD analysis was employed to study the structural features of prepared powders. As can be seen in Figure 3, XRD results corroborate with those obtained by IR spectroscopy. The patterns of all samples exhibited a slight bump indicating the presence of an amorphous network along with diffraction pics corresponding to calcium carbonate and calcium oxide phases. The calcium carbonate phase is highlighted by the peaks at 29.3°, 39.2° and the doublet at 47.4 and 48.3° which are attributed to diffraction of (104) (113) (018) and (116) plans, respectively [47]. These peaks suggest that the calcium carbonate is in the form of calcite phase [48]. Additionally, the peaks at 32°, 39°, and 53.7° can be assigned to diffraction plans relative to crystalline calcium oxide. It is suggested that the presence of calcium oxide phase arose from the partial decomposition of calcium carbonate. During calcination, a fraction of calcium carbonate crystals decomposed to generate calcium oxide. The TGA results are found to be congruent with the

Table 3: ICP-AES results of all samples presented in (g/g sample). *Theo*: theoretical values; *Exp*: experimental values [16]

Glass composition	*Si*	*Ca*	*P*	*Ta*
	Theo | *Exp* ($g.g^{-1}$)	*Theo* | *Exp* ($g.g^{-1}$)	*Theo* | *Exp* ($g.g^{-1}$)	*Theo* | *Exp* ($g.g^{-1}$)
58S	0.2598 | 0.2630	0.2364 | 0.2427	0.0493 | 0.0471	0 | 0
58S0.2	0.2573 | 0.2495	0.2341 | 0.2469	0.0469 | 0.04402	0.0114 | 0.0125
58S0.4	0.2549 | 0.2598	0.2319 | 0.2356	0.0445 | 0.0457	0.0226 | 0.0219
58S0.6	0.2526 | 0.2486	0.2298 | 0.2196	0.0422 | 0.0427	0.0336 | 0.0345
58S0.8	0.2502 | 0.2574	0.2277 | 0.2335	0.0399 | 0.0410	0.0444 | 0.0439
58S1	0.2480 | 0.2459	0.2256 | 0.2170	0.0376 | 0.038	0.0550 | 0.0563

XRD findings where diffraction peaks of $CaCO_3$ and CaO were both detected. It is also important to mention that the calcination was carried out at 600°C. At this temperature, structural changes may have occurred, explaining the results observed by XRD and TGA analysis. Anand *et al.* [49] accomplished the synthesis of three mesoporous bioactive glasses (MBG) by varying the composition and surfactant. They found that, for P123 synthesized MBG, crystallization of calcium carbonate and hydroxyapatite occured. Fernando *et al.* [50] used acetate precursors for calcium and sodium to synthesize a series of MBGs. By changing the calcination temperature of samples, they found that the calcium carbonate phase was initially formed when calcination was conducted at 380°C. Their results suggested that calcite formation in mesoporous bioactive glasses is mainly caused by the surfactant degradation. During calcination, two main phenomena may have occurred. The decomposition of the surfactant molecules and the diffusion of the network modifiers cations into the silica network. Pluronic molecules are decomposed to provide primarily carbone dioxide. In the presence of water vapor, carbonate ions can be formed through the dissolution of CO_2 molecules. In this sense, the compensation of charge is an important factor to take into consideration. Necessary counter-ions may be supplied from the decomposition products of the organic phase [51]. Perardi *et al.* [52] studied the carbonate formation on 58S and 45S5 compositions. Their results indicated that the reactivity of Ca^{2+} species along with the surface area, the presence of CO_2 and excess of water have led to fast carbonate formation especially in the case of 58S. For these reasons, it is assumed that the nuclei of $CaCO_3$ are formed. Consequently, the growth of the carbonate phase will follow up by consuming the abandon calcium cations present in the structure and carbonate ions originated from the decomposition of the surfactant molecules.

The results of the ICP analysis are depicted in Table 3. The sample concentrations are presented as the mass of each element (in g) per gram of samples. For all samples, the experimental values, obtained through ICP analysis, correspond to the theoretical ones with the existence of slight deviations.

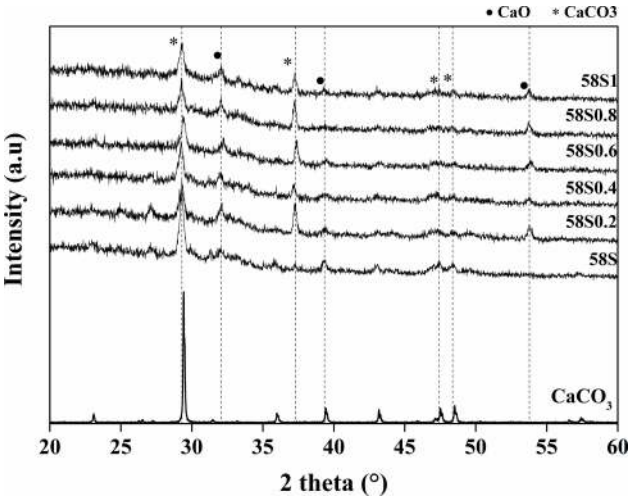

Figure 3: XRD spectra of samples after calcination at 600°C

The microstructure of prepared glasses was assessed by SEM and the resulted images are presented in Figure 4 along with their EDX spectra. SEM images indicate the presence of grains with various shapes and sizes, fully or partially covered with smaller particles. it is assumed that the grains correspond to the glassy silicate phase whereas the covering particles can be attributed to calcium carbonate crystals. The results showed that a part of calcium did not enter the glass structure as network modifier and was converted to calcium carbonate as was inferred from the structural characterization. Additionally, EDX spectra indicate the presence of tantalum in the doped powders. This result is highlighted by the presence of the $M\alpha_1$ peak at 1.712 keV.

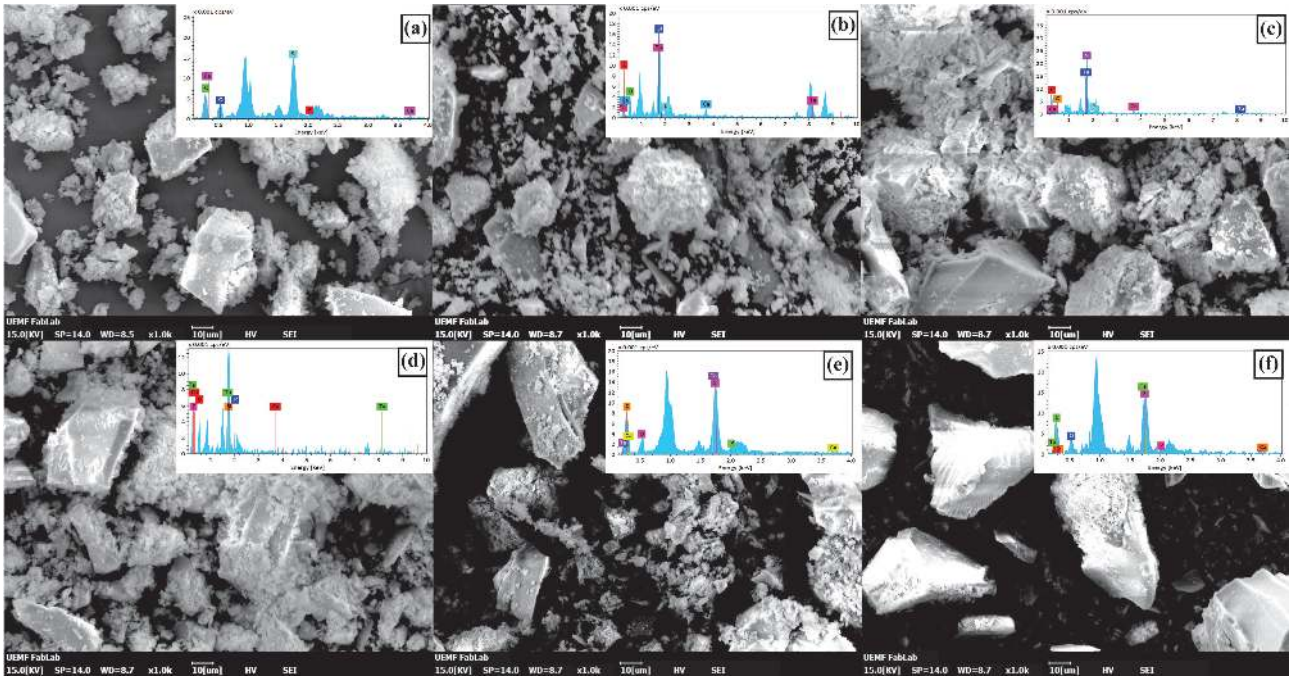

Figure 4: SEM images of powders in the 58S-Ta series (a: 58S; b: 58S0.2Ta; c: 58S0.4Ta. d: 58S0.6Ta; e: 58S0.8Ta; f: 58S1Ta)

3.2 *In vitro* bioactivity

The assessment of *in vitro* acellular bioactivity of the 58S-Ta series was carried out through SBF test. The corresponding FTIR spectra are displayed in Figure 5. The spectra reveal a common behavior of bioactive material with the apparition of two new peaks relative to P-O vibrations. These peaks can be detected after only 6 hours of immersion and can be identified for all compositions. The result suggest that present materials can generate calcium phosphate-rich crystalline layers on their surface through immersion in simulated body fluid. Other changes in the FTIR spectra can be noticed. The intensity of carbonate peaks at 1414 and 870 cm^{-1} decreases with immersion time and these peaks are still identified even after 14 days in SBF. This probably means that the dissolution of calcium carbonate had occurred, thus, increasing the concentration of calcium and carbonate ions in the medium. Additionally, the Si-OH related band decreased in intensity and a new peak relative to P-O vibration is detected at 960 cm^{-1}. Following the bioactivity mechanisms suggested by Hench *et al.* [31], it can be hypothesized that condensation of silanol groups occurred and a formation of a silica-rich layer was formed in the early stages of *in vitro* bioactivity. FTIR results showed promising results regarding the bioactivity of our glass powders. The development of P-O crystalline pics after only 6 hours of *in vitro* bioactivity test suggested that the partial crystallization that occurred during calcination did not slow down the rate of the bioactive response.

XRD analysis was conducted to further monitor the changes induced by the immersion of prepared glasses in SBF. The spectra in Figure 6 present the results of XRD after 6 hours and 7 days in SBF for all compositions. Firstly, the characteristic band relative to amorphous materials are more pronounced after 6 hours in SBF. Secondly, the peaks relative to $CaCO_3$ decreased in intensity as a function of immersion time, suggesting its dissolution when in contact with the SBF solution. Finally, new characteristic peaks at 26°C and 32° had developed after 6 hours of treatment. These peaks, which are relative to diffraction of plans (002) and (211) in hydroxyapatite became more intense after 7 days in SBF immersion [47]. Comparing these results, and taking into account Ta molar fraction, it can be concluded that the presence of tantalum at 0.8 and 1% moles had slowed down the formation of hydroxyapatite, judging from the intensity of the new peaks relative to HA, whereas for low or medium percentages its presence enhanced the bioactivity.

As in any complex system, understanding the phenomena that occur will allow the understanding of the most influential parameters. In our case, the bioactivity is thought to be impacted by the presence of calcium carbonate and the variation of the tantalum content in the glass composition. Regarding the presence of calcium carbonate, it was inferred by previous studies that a dissolution-

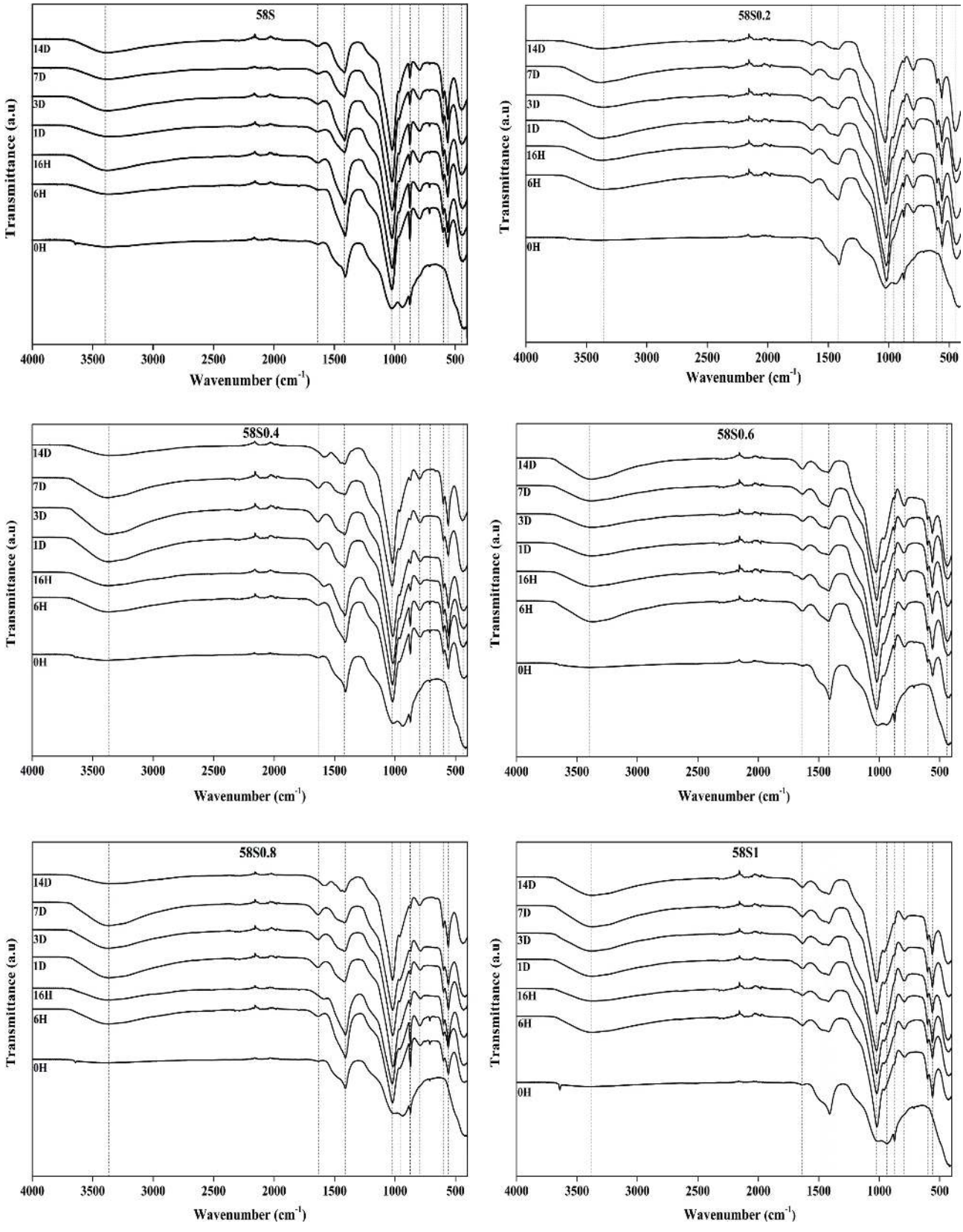

Figure 5: FTIR analysis of samples after various periods in SBF

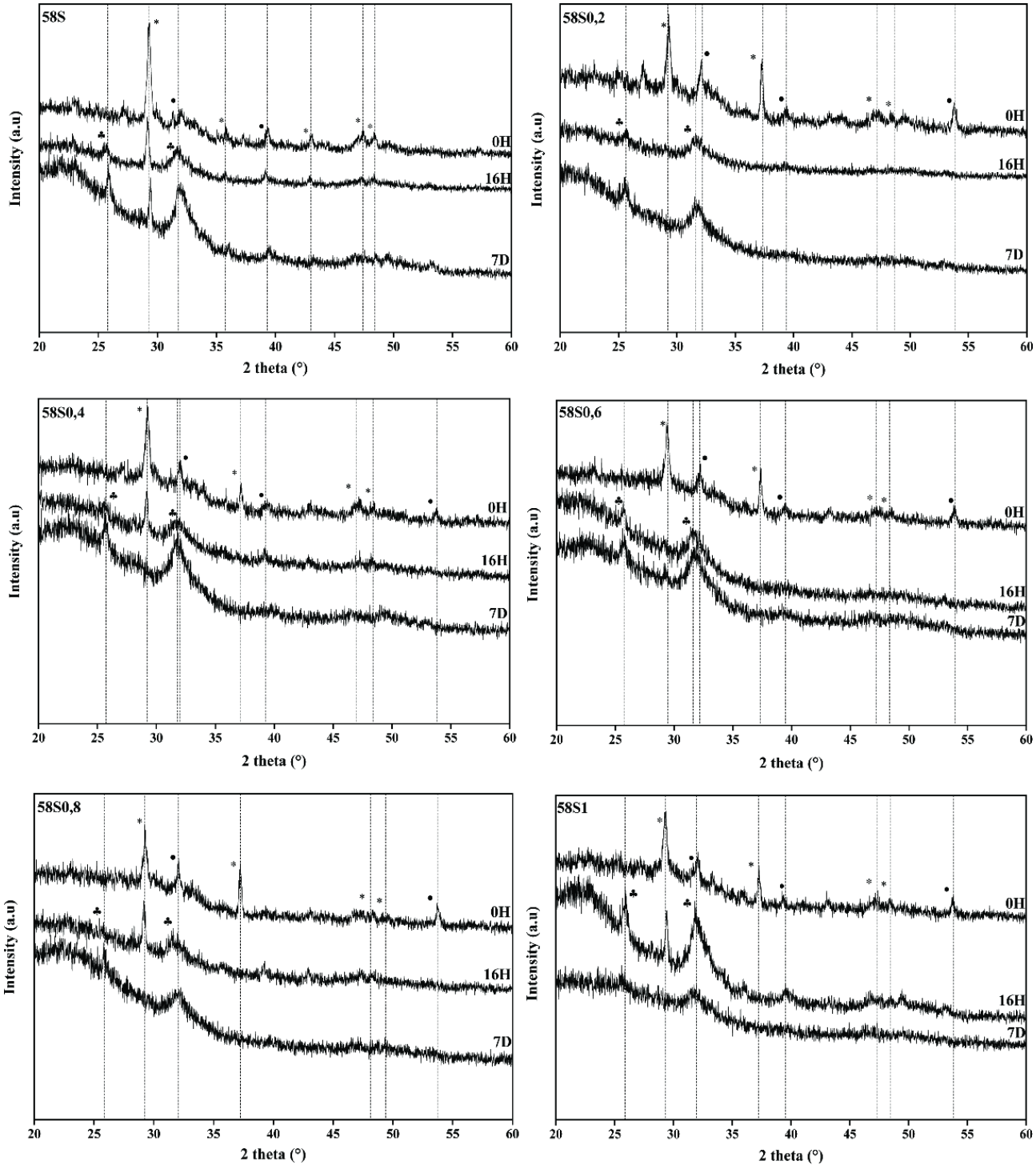

Figure 6: XRD results of powders in the 58S-Ta series after immersion in SBF for 6 hours and 7 days

recrystallization mechanism occurred when the carbonate phase is immersed in a phosphate-rich solution at room temperature [53, 54]. A dissolution occurred first in which calcium and carbonate ions are leached into the solution. Then precipitation of the apatite phase takes place when the phosphate ions react with the calcium ions in the solution. In a recent study, Myszka *et al.* showed that the formation of the Ca-P layer, through the SBF test, on calcium carbonates is phase-dependent [55]. They demonstrated that calcite is bioinert and that the bioactivity of calcium carbonate increased with increasing polymorph solubility. It is known that the solubility of calcite is lower than

that of aragonite and vaterite. With lower solubility, the calcite phase became less degradable, which slowed the leaching of ions into the surrounding medium [56]. In our study, *in vitro* acellular bioactivity was well demonstrated through FTIR and XRD for the entire 58S-Ta series. It was shown that calcium carbonate presence did not alter the powders' bioactivity. We believe that it can be favorable for rapid apatite precipitation and, eventually, for bone bonding [57, 58].

Regarding tantalum, our results showed that hydroxyapatite formation began to decrease when Ta_2O_5 increases over 0.6% mol. In this sense, the presence of tantalum has a favorable effect on glass bioactivity in lower molar fractions, whereas, for higher tantalum content, it showed a retardation effect on the precipitation of the apatite phase, thus on bioactivity. It was also reported that metallic oxide can play the role of network formers or network modifiers based on their concentration. For low concentration, they can enter the network as modifiers creating non-bridging oxygen and disrupting the silica network. Whereas for high concentration they can act as network formers creating more bridging oxygen.

Figure 7 showed variations of pH for the Ta-58S series after the SBF test. The results indicated that after 14 days of immersion in SBF, the pH of the solution was highest for 0.2, 0.4 and 0.6% mol with a value of 7.9 whereas it decreases at 0.8 and 1% at a value of 7.86 and 7.77 respectively. We hypothesis that for Ta_2O_5 content below 0.6%, Ta acts as a network modifier. This will increase the solubility of glass, which in turn will enhance its reactivity. Additionally, higher pH values are favorable for hydroxyapatite precipitation. For higher doping content, tantalum may act as a network former. This will lead to a decrease in glass solubility and subsequently decrease the rate of HA precipitation. Alhalawani *et al.* [37] studied the impact of substituting the zinc with tantalum in a multi-component silicate glass. Their results showed that the number of bridging oxygen increased with increasing tantalum content. SEM images after 7 days of the bioactivity tests are presented in Figure 8. It can be seen that the morphology of the covering material had changed. Images show the growth of a new phase which can be attributed to hydroxyapatite. The results also suggested the dissolution of calcium carbonate phase after immersion in the SBF solution.

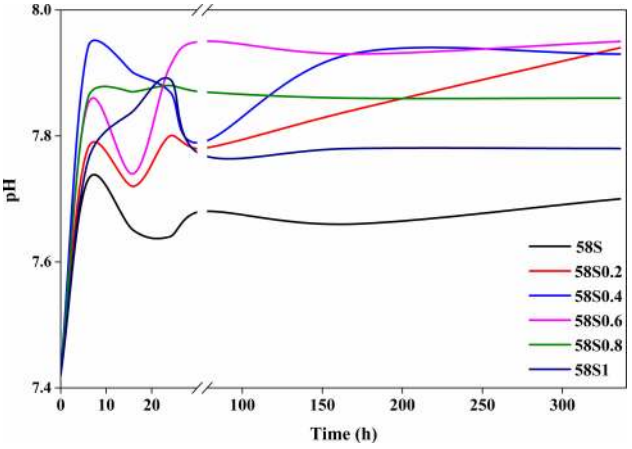

Figure 7: Variations of pH after different periods in SBF for all samples in the 58S-Ta series

3.3 Antibacterial activity

The antibacterial activities of the 58S and Ta-58S bioactive glasses were evaluated by the plate counting method. The antibacterial activity was tested against *Staphylococcus aureus* (Gram-positive) and *Escherichia coli* (Gram-negative), due to their involvement in nosocomial infections in orthopedic implant surgery [59]. Figure 9 showed that bioglass with Ta content strongly decreased the cell viability of *E. coli* bacteria compared to the 58S bioglass. It was concluded that tantalum ion inhibited the growth of gram-negative bacteria. The same figure also demonstrated the effect of the synthesized bioglass on *S. aureus*. It was observed that the viability of *S. aureus* was significantly reduced to a low percentage of approximately 9% for 58S0.8 and 58S1 samples, which indicates the antibacterial effect of the 58S bioglass doped tantalum. The results showed that the cell viability of *E. coli* and *S. aureus* decreases with increasing Ta content in the composition. However, this effect is more pronounced in the case of S. aureus. Regarding the undoped composition, it presented a negative effect including any inhibition of bacteria growth, as it is highlighted by Figure 10 and 11. The cell viability was 99% and 88% for *E. coli* and *S. aureus* respectively. We can conclude that 58S bioglass doped tantalum possessed antibacterial effects against gram-positive and gram-negative bacteria.

It has been described in the literature that tantalum can have an inhibition effect on bacteria growth and adhesion. Guo *et al.* have shown that doping ZnO nanoparticles with tantalum ions resulted in improved antibacterial activity against *E. coli* and *S. aureus* [60]. They showed that these nanoparticles were able to create some holes in membrane cells, resulting in a loss of minerals, proteins and genetic materials causing the cells apoptosis. Another study has revealed that the introduction of tantalum ions, as a doping element in a ceramic matrix, exhibited an inhibition effect on the growth of gram-positive bacteria only [61]. It has been reported that the increase of the

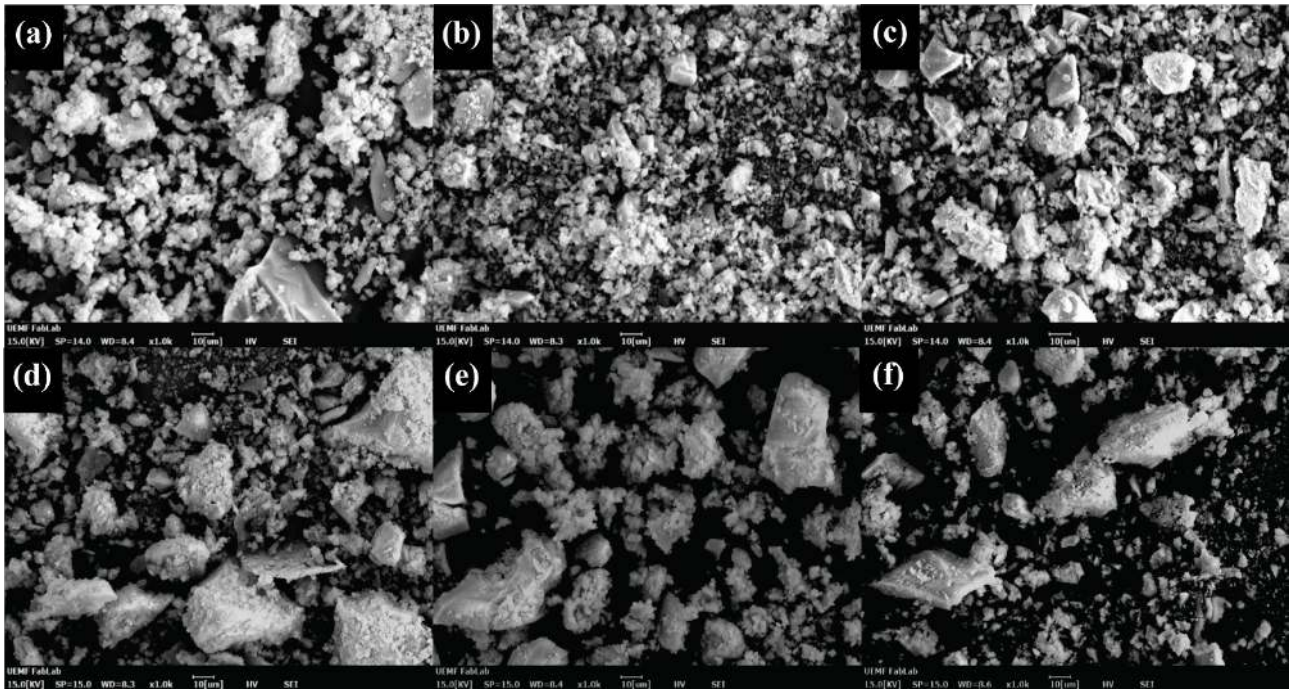

Figure 8: SEM images of powders in the 58S-Ta series after 7 days of immersion in SBF (a: 58S; b: 58S0.2Ta; c: 58S0.4Ta. d: 58S0.6Ta; e: 58S0.8Ta; f: 58S1Ta)

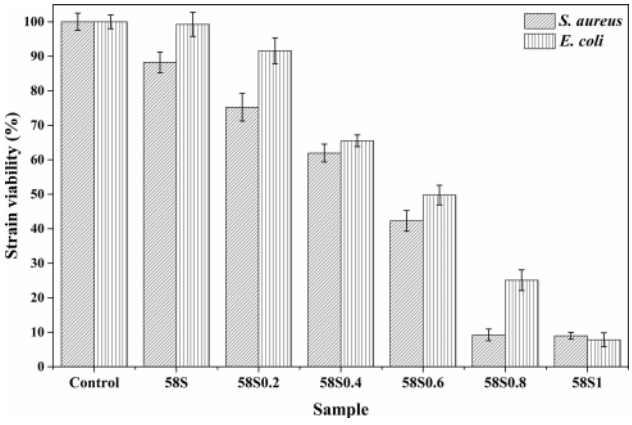

Figure 9: Antibacterial activity of the 58S-Ta series presented as cells viability of E. coli and S. aureus

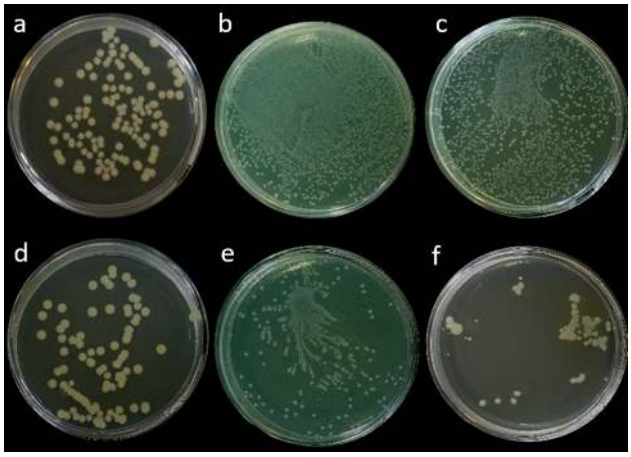

Figure 10: Images illustrating the growth of E. coli with and without samples; a, b and c: controls for 58S, 58S0.6 and 58S1, respectively; d, e and f: growth of bacteria in the presence of samples 58S, 58S0.6 and 58S1, respectively

Ta^{+5}-ion concentration hinders the bacteria growth by the creation of a hyperosmotic environment due to its high ionic strength [62]. A recent study by Yang *et al.* have found that tantalum film displayed no favorable antibacterial responses *in vitro* against *E. coli* [63]. Nevertheless, *in vivo* mouse soft tissue infection test and further *ex vivo* studies, have shown that tantalum displayed antibacterial activity. Thus, it was hypothesized that tantalum ions act as immune-stimulator agents where the performance of innate immunity cells like macrophages and neutrophils is enhanced.

In the present study, we demonstrate that our tantalum doped bioglass possesses high antibacterial activity against gram-negative and gram-positive bacteria. We hypothesize that the released tantalum ions adhere to the cell membrane, causing a malfunction of the bacteria that leads eventually to its death. Moreover, the antibacterial activity can also be related to the generation of oxygen reactive species (ROS) affecting the metabolic processes, in-

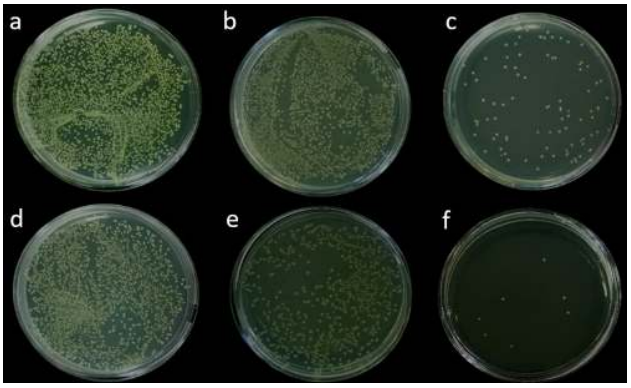

Figure 11: Images illustrating the growth of S. aureus with and without samples; a, b and c: controls for 58S, 58S0.6 and 58S1, respectively; d, e and f: growth of bacteria in the presence of samples 58S, 58S0.6 and 58S1, respectively

cluding DNA replication. This behavior is comparable to that of metallic ions, such as Zn^{2+}, Cu^{2+}, and Ag^{+}, as they enter the metabolic system of bacteria causing the formation of toxic secondary metabolites and leading to the microorganism's death [64]. This assumption is consistent with literature data performed by Russo *et al.* [64], and reported that CuTCP particles showed a growth inhibition of *S. aureus* and *E. coli*, based on copper dissolution in the medium, leading to cell membrane rupture, reactive oxygen species production and plasmid DNA degradation, which induce cell apoptosis.

In previous work, it was noted that pH value plays a key role in antibacterial performance. As it is well-known glass dissolution result in leaching of alkaline ions into the medium that subsequently lead to pH increase. Allan *et al.* [65] have shown that to have antibacterial activity, the medium pH should reach a value comprised between 8.9 and 9.8. In the bioactivity study, we showed that pH value did not exceed a value of 8 even after 14 days of contact, for all compositions. Based on this, we suggest that the main factor responsible for the antibacterial activity of Ta doped bio-ceramics is the inherent presence of tantalum ions rather than the increase of the pH of the medium. Another study, investigated by Kawakami *et al.* on the antibacterial activity of several pure metals using the JIS Z 2801 standard test against *E. coli* and *S. aureus* [66]. They showed that, except for molybdenum, the range of pH during the experiment for all other metals, including tantalum, was between 6 and 7.5 only, this is in agreement with our observations [67]. Some studies on the antibacterial activity of bioactive glasses reported that the very high pH value was the most determining factor in inhibiting bacteria growth [65, 68]. Nevertheless, this increase can also have a toxic effect on other cells [69]. Hence, our bioactive glasses doped with tantalum, synthesized in this work, present a good combination with bioactivity and intrinsic antibacterial activity against *E. coli* and *S. aureus*, rendering them promising candidates for bone regeneration applications.

4 Conclusion

In this work, we report the synthesis and characterization of a series of bioactive glasses doped with tantalum, with different percentage. The structural assessment showed the existence of a second phase which was identified to be calcite. This phase originated from the calcination phase in which the structural directing agent was removed. Bioactivity study indicated that doping with tantalum enhanced apatite forming ability of glasses for concentration below 0.6% whereas for higher concentration it had a retardation effect. Antibacterial test against *E. coli* and *S. aureus* showed that tantalum incorporation had an inhibition effect on the growth of the two bacteria. This effect was more pronounced for Ta_2O_5 concentration above 0.6% mol. Therefore, we suggest that the 58S0.6 composition can be a good candidate as a multifunctional bioceramic for bone tissue regeneration.

Acknowledgement: Authors address their acknowledgements to the National Center of Scientific and Technological Research, CNRST (Rabat, Morocco), the Regional Council Fes-Meknes and the Euromed University of Fes for supporting the present work.

Ethical approval: The conducted research is not related to either human or animals use.

Conflict of Interests: The authors declare no conflict of interest regarding the publication of this paper.

References

[1] Li J.J., Kaplan D.L., Zreiqat H., Scaffold-based regeneration of skeletal tissues to meet clinical challenges, J. Mater. Chem. B, 2014, 2, 7272-7306.
[2] Hench L.L., Chronology of Bioactive Glass Development and Clinical Applications, New J. Glas. Ceram., 2013, 03, 67-73.
[3] Hench L.L., The story of Bioglass®, J. Mater. Sci. Mater. Med., 2006, 17, 967-978.
[4] Li R., Clark A.E., Hench L.L., An investigation of bioactive glass powders by sol-gel processing, J. Appl. Biomater., 1991, 2, 231-239.

[5] Yan X., Yu C., Zhou X., Tang J., Zhao D., Highly ordered mesoporous bioactive glasses with superior in vitro bone-forming bioactivities, Angew. Chemie - Int. Ed., 2004, 43, 5980-5984.
[6] Lo'pez-Noriega A., Arcos D., Izquierdo-Barba I., Sakamoto Y., Terasaki O., Vallet-Regı M., Ordered mesoporous bioactive glasses for bone tissue regeneration, Chem. Mater., 2006, 18, 3137-3144.
[7] Knabe C., Adel-Khattab D., Ducheyne P., 1.12 Bioactivity: Mechanisms, Compr. Biomater. II, 2017, 1, 291-310.
[8] Singh A., Dubey A.K., Various Biomaterials and Techniques for Improving Antibacterial Response, ACS Appl. Bio Mater., 2018, 1, 3-20.
[9] Fernandes J.S., Gentile P., Pires R.A., Reis R.L., Hatton P. V., Multifunctional bioactive glass and glass-ceramic biomaterials with antibacterial properties for repair and regeneration of bone tissue, Acta Biomater., 2017, 59, 2-11.
[10] Arciola C.R., Campoccia D., Montanaro L., Implant infections: Adhesion, biofilm formation and immune evasion, Nat. Rev. Microbiol., 2018, 16, 397-409.
[11] Eng A.S., Eng E.T., Eng F.P., Prof A.R.B., Recent progress in inorganic and composite coatings with bactericidal capability for orthopaedic applications, Nanomedicine Nanotechnology, Biol. Med., 2011, 7, 22-39.
[12] Johnson C.T., García A.J., Scaffold-based Anti-infection Strategies in Bone Repair, Ann. Biomed. Eng., 2015, 43, 515-528.
[13] Bordi C., de Bentzmann S., Hacking into bacterial biofilms: a new therapeutic challenge, Ann. Intensive Care, 2011, 1, 1-8.
[14] Nathan C., Cars O., Antibiotic Resistance — Problems, Progress, and Prospects, N. Engl., 2014, 689-691.
[15] Cacciotti I., Bivalent cationic ions doped bioactive glasses: the influence of magnesium, zinc, strontium and copper on the physical and biological properties, J. Mater. Sci., 2017, 52, 8812-8831.
[16] Tabia Z., El Mabrouk K., Bricha M., Nouneh K., Mesoporous bioactive glass nanoparticles doped with magnesium: drug delivery and acellular in vitro bioactivity, RSC Adv., 2019, 9, 12232-12246.
[17] Daguano J.K.M.F., Rogero S.O., Crovace M.C., Peitl O., Strecker K., Dos Santos C., Bioactivity and cytotoxicity of glass and glass-ceramics based on the $3CaO{\cdot}P_2O_5$-SiO_2-MgO system, J. Mater. Sci. Mater. Med., 2013, 24, 2171-2180.
[18] Romero-Gavilán F., Araújo-Gomes N., García-Arnáez I., Martínez-Ramos C., Elortza F., Azkargorta M., Iloro I., Gurruchaga M., Suay J., Goñi I., The effect of strontium incorporation into sol-gel biomaterials on their protein adsorption and cell interactions, Colloids Surfaces B Biointerfaces, 2019, 174, 9-16.
[19] Rau J. V., Curcio M., Raucci M.G., Barbaro K., Fasolino I., Teghil R., Ambrosio L., De Bonis A., Boccaccini A.R., Cu-Releasing Bioactive Glass Coatings and Their in Vitro Properties, ACS Appl. Mater. Interfaces, 2019, 11, 5812-5820.
[20] Sharifianjazi F., Parvin N., Tahriri M., Synthesis and characteristics of sol-gel bioactive SiO_2-P_2O_5-CaO-Ag_2O glasses, J. Non. Cryst. Solids, 2017, 476, 108-113.
[21] Brückner R., Tylkowski M., Hupa L., Brauer D.S., Controlling the ion release from mixed alkali bioactive glasses by varying modifier ionic radii and molar volume, J. Mater. Chem. B, 2016, 4, 3121-3134.
[22] Lao J., Jallot E., Nedelec J.M., Strontium-delivering glasses with enhanced bioactivity: A new biomaterial for antiosteoporotic applications?, Chem. Mater., 2008, 20, 4969-4973.
[23] Gentleman E., Fredholm Y.C., Jell G., Lotfibakhshaiesh N., O'Donnell M.D., Hill R.G., Stevens M.M., The effects of strontium-substituted bioactive glasses on osteoblasts and osteoclasts in vitro, Biomaterials, 2010, 31, 3949-3956.
[24] Isaac J., Nohra J., Lao J., Jallot E., Nedelec J.M., Berdal A., Sautier J.M., Effects of strontium-doped bioactive glass on the differentiation of cultured osteogenic cells, Eur. Cells Mater., 2011, 21, 130-143.
[25] Romero-Sánchez L.B., Marí-Beffa M., Carrillo P., Medina M.Á., Díaz-Cuenca A., Copper-containing mesoporous bioactive glass promotes angiogenesis in an in vivo zebrafish model, Acta Biomater., 2018, 68, 272-285.
[26] Zhu H., Hu C., Zhang F., Feng X., Li J., Liu T., Chen J., Zhang J., Preparation and antibacterial property of silver-containing mesoporous 58S bioactive glass, Mater. Sci. Eng. C, 2014, 42, 22-30.
[27] Zheng K., Balasubramanian P., Paterson T., Stein R., MacNeil S., Fiorilli S., Vitale-Brovarone C., Shepherd J., Boccaccini A.R., Ag modified mesoporous bioactive glass nanoparticles for enhanced antibacterial activity in 3D infected skin model, Mater. Sci. Eng. C, 2019, 103, 109764.
[28] Pourshahrestani S., Zeimaran E., Kadri N.A., Gargiulo N., Jindal H.M., Naveen S.V., Sekaran S.D., Kamarul T., Towler M.R., Potency and Cytotoxicity of a Novel Gallium-Containing Mesoporous Bioactive Glass/Chitosan Composite Scaffold as Hemostatic Agents, ACS Appl. Mater. Interfaces, 2017, 9, 31381-31392.
[29] Goh Y.F., Alshemary A.Z., Akram M., Abdul Kadir M.R., Hussain R., In-vitro characterization of antibacterial bioactive glass containing ceria, Ceram. Int., 2014, 40, 729-737.
[30] Alhalawani A.M.F., Towler M.R., The effect of ZnO-Ta_2O_5 substitution on the structural and thermal properties of SiO_2-ZnO-SrO-CaO-P_2O_5 glasses, Mater. Charact., 2016, 114, 218-224.
[31] George N., Nair A.B., Porous tantalum, Elsevier Ltd, 2018,.
[32] Shi L.Y., Wang A., Zang F.Z., Wang J.X., Pan X.W., Chen H.J., Tantalum-coated pedicle screws enhance implant integration, Colloids Surf. B Biointerf, 2017, 160, 22-32.
[33] Ma Z., Xie H., Wang B., Wei X., Zhao D., A novel Tantalum coating on porous SiC used for bone filling material, Mater. Lett., 2016, 179, 166-169.
[34] Levine B.R., Sporer S., Poggie R.A., Della Valle C.J., Jacobs J.J., Experimental and clinical performance of porous tantalum in orthopedic surgery, Biomaterials, 2006, 27, 4671-4681.
[35] Stanic V., Nicoli Aldini N., Fini M., Giavaresi G., Giardino R., Krajewski A., Ravaglioli A., Mazzocchi M., Dubini B., Ponzi Bossi M.G., Rustichelli F., Osteointegration of bioactive glass-coated zirconia in healthy bone: An in vivo evaluation, Biomaterials, 2002, 23, 3833-3841.
[36] Rosengren Å., Oscarsson S., Mazzocchi M., Krajewski A., Ravaglioli A., Protein adsorption onto two bioactive glass-ceramics, Biomaterials, 2003, 24, 147-155.
[37] Alhalawani A.M., Towler M.R., A novel tantalum-containing bioglass. Part I. Structure and solubility, Mater. Sci. Eng. C, 2017, 72, 202-211.
[38] Cordeiro L., Silva R.M., De Pietro G.M., Pereira C., Ferreira E.A., Ribeiro S.J.L., Messaddeq Y., Cassanjes F.C., Poirier G., Thermal and structural properties of tantalum alkali-phosphate glasses, J. Non. Cryst. Solids, 2014, 402, 44-48.
[39] Lombardi M., Cacciotti I., Bianco A., Montanaro L., RKKP bioactive glass-ceramic material through an aqueous sol-gel process, Ceram. Int., 2015, 41, 3371-3380.
[40] Russo T., de Santis R., Gloria A., Barbaro K., Altigeri A., Fadeeva I. V, Rau J. V, Modification of PMMA cements for cranioplasty with bioactive glass and copper doped tricalcium phosphate particles,

Polymers (Basel)., 2020, 12, 4-6.
[41] Rau J. V., Teghil R., Fosca M., De Bonis A., Cacciotti I., Bianco A., Albertini V.R., Caminiti R., Ravaglioli A., Bioactive glass-ceramic coatings prepared by pulsed laser deposition from RKKP targets (sol-gel vs melt-processing route), Mater. Res. Bull., 2012, 47, 1130-1137.
[42] Mendonca A., Rahman S., Alhalawani A., Rodriguez O., Gallant R.C., Ni H., Clarkin O.M., Towler M.R., The effect of tantalum incorporation on the physical and chemical properties of ternary silicon - calcium - phosphorous mesoporous bioactive glasses, J. Biomed. Mater. Res. Part B Appl. Biomater., 2019, 000B, 1-9.
[43] Kokubo T., Takadama H., How useful is SBF in predicting in vivo bone bioactivity?, Biomaterials, 2006, 27, 2907-2915.
[44] Hu S., Chang J., Liu M., Ning C., Study on antibacterial effect of 45S5 Bioglass®, J. Mater. Sci. Mater. Med., 2009, 20, 281-286.
[45] Bérubé F., Kaliaguine S., Calcination and thermal degradation mechanisms of triblock copolymer template in SBA-15 materials, Microporous Mesoporous Mater., 2008, 115, 469-479.
[46] Filgueiras M.R.T., La Torre G., Hench L.L., Solution effects on the surface reactions of three bioactive glass compositions, J. Biomed. Mater. Res., 1993, 27, 1485-1493.
[47] Mozafari M., Moztarzadeh F., Tahriri M., Investigation of the physico-chemical reactivity of a mesoporous bioactive SiO_2-CaO-P_2O_5 glass in simulated body fluid, J. Non. Cryst. Solids, 2010, 356, 1470-1478.
[48] Kontoyannis C.G., Vagenas N. V, Calcium Carbonate Phase Analysis Using XRD and FT - Raman Spectroscopy Calcium carbonate phase analysis using XRD and FT-Raman spectroscopy, Analyst, 2015, 125, 251-255.
[49] Anand A., Lalzawmliana V., Kumar V., Das P., Devi K.B., Maji A.K., Kundu B., Roy M., Nandi S.K., Preparation and in vivo biocompatibility studies of different mesoporous bioactive glasses, J. Mech. Behav. Biomed. Mater., 2019, 89, 89-98.
[50] Fernando D., Attik N., Cresswell M., Mokbel I., Pradelle-Plasse N., Jackson P., Grosgogeat B., Colon P., Influence of network modifiers in an acetate based sol-gel bioactive glass system, Microporous Mesoporous Mater., 2018, 257, 99-109.
[51] Kleitz F., Schmidt W., Schüth F., Calcination behavior of different surfactant-templated mesostructured silica materials, Microporous Mesoporous Mater., 2003, 65, 1-29.
[52] Perardi A., Cerrruti M., Morterra C., Carbonate formation on sol-gel bioactive glass 58S and on Bioglass® 45S5, Stud. Surf. Sci. Catal., 2005, 155, 461-469.
[53] Cruz M.A.E., Ruiz G.C.M., Faria A.N., Zancanela D.C., Pereira L.S., Ciancaglini P., Ramos A.P., Calcium carbonate hybrid coating promotes the formation of biomimetic hydroxyapatite on titanium surfaces, Appl. Surf. Sci., 2016, 370, 459-468.
[54] Guo Y.P., Zhou Y., Conversion of nacre powders to apatite in phosphate buffer solutions at low temperatures, Mater. Chem. Phys., 2007, 106, 88-94.
[55] Myszka B., Hurle K., Demmert B., Detsch R., Boccaccini A.R., Wolf S.E., Phase-specific bioactivity and altered Ostwald ripening pathways of calcium carbonate polymorphs in simulated body fluid, RSC Adv., 2019, 9, 18232-18244.
[56] He F., Zhang J., Tian X., Wu S., Chen X., A facile magnesium-containing calcium carbonate biomaterial as potential bone graft, Colloids Surfaces B Biointerfaces, 2015, 136, 845-852.
[57] Zhang Y., Wang J., Sharma V.K., Designed synthesis of hydroxyapatite nanostructures: Bullet-like single crystal and whiskered hollow ellipsoid, J. Mater. Sci. Mater. Med., 2014, 25, 1395-1401.
[58] Mozafari M., Banijamali S., Baino F., Kargozar S., Hill R.G., Calcium carbonate: Adored and ignored in bioactivity assessment, Acta Biomater., 2019, 91, 35-47.
[59] Barth E., Myrvik Q.M., Wagner W., Gristina A.G., In vitro and in vivo comparative colonization of Staphylococcus aureus and Staphylococcus epidermidis on orthopaedic implant materials, Biomaterials, 1989, 10, 325-328.
[60] Kong J.-Z., Wu D., Li A.-D., Cao Y.-Q., Han P., Guo B.-L., Guo L.-C., Zhai H.-F., The Antibacterial Activity of Ta-doped ZnO Nanoparticles, Nanoscale Res. Lett., 2015, 10, 336.
[61] Riaz M., Zia R., Saleemi F., Hussain T., In Vitro antibacterial activity of Ta2O5 doped glass-ceramics against pathogenic bacteria, J. Alloys Compd., 2018, 764, 10-16.
[62] Harrison P.L., Harrison T., Stockley I., Smith T.J., Does tantalum exhibit any intrinsic antimicrobial or antibiofilm properties?, Bone Jt. J., 2017, 99B, 1153-1156.
[63] Yang C., Li J., Zhu C., Zhang Q., Yu J., Wang J., Wang Q., Tang J., Zhou H., Shen H., Advanced Antibacterial Activity of Biocompatible Tantalum Nanofilm via Enhanced Local Innate Immunity, Acta Biomater., 2019, 89, 403-418.
[64] Chudobova D., Dostalova S., Ruttkay-Nedecky B., Guran R., Rodrigo M.A.M., Tmejova K., Krizkova S., Zitka O., Adam V., Kizek R., The effect of metal ions on Staphylococcus aureus revealed by biochemical and mass spectrometric analyses, Microbiol. Res., 2015, 170, 147-156.
[65] Allan I., Newman H., Wilson M., Antibacterial activity of particulate Bioglass® against supra- and subgingival bacteria, Biomaterials, 2001, 22, 1683-1687.
[66] Kawakami H., Yoshida K., Nishida Y., Kikuchi Y., Sato Y., Antibacterial Properties of Metallic Elements for Alloying Evaluated with Application of JIS Z 2801:2000, ISIJ Int., 2008, 48, 1299-1304.
[67] Life F.A., Microbial Ecology of Foods, Microb. Ecol. Foods, 2016.
[68] Munukka E., Yla H., Viljanen M.K., Zhang D., Leppa O., Antibacterial effects and dissolution behavior of six bioactive glasses, J. Biomed. Mater. Res. Part A, 2009, 93, 475-483.
[69] Ciraldo F.E., Boccardi E., Melli V., Westhauser F., Boccaccini A.R., Tackling bioactive glass excessive in vitro bioreactivity: Preconditioning approaches for cell culture tests, Acta Biomater., 2018, 75, 3-10.